

# Analyst

Accepted Manuscript



This is an *Accepted Manuscript*, which has been through the Royal Society of Chemistry peer review process and has been accepted for publication.

*Accepted Manuscripts* are published online shortly after acceptance, before technical editing, formatting and proof reading. Using this free service, authors can make their results available to the community, in citable form, before we publish the edited article. We will replace this *Accepted Manuscript* with the edited and formatted *Advance Article* as soon as it is available.

You can find more information about *Accepted Manuscripts* in the [Information for Authors](#).

Please note that technical editing may introduce minor changes to the text and/or graphics, which may alter content. The journal's standard [Terms & Conditions](#) and the [Ethical guidelines](#) still apply. In no event shall the Royal Society of Chemistry be held responsible for any errors or omissions in this *Accepted Manuscript* or any consequences arising from the use of any information it contains.

1  
2  
3 **Article type: Communication**  
4

5 **Title:** An amorphous silicon photodiode microfluidic chip to detect nanomolar quantities of  
6 HIV-1 virion infectivity factor  
7

8  
9 **Authors:** Cláudia R. Vistas<sup>a</sup>, Sandra S. Soares<sup>a</sup>, Rogério M. M. Rodrigues<sup>a</sup>, Virginia Chu<sup>b</sup>,  
10 João P. Conde<sup>b,c</sup>, Guilherme N. M. Ferreira<sup>a</sup>  
11

12  
13 <sup>a</sup> IBB-Institute for Biotechnology and Bioengineering, Centre for Molecular and Structural  
14 Biomedicine (CBME), University of Algarve, Campus de Gambelas, 8000-139 Faro,  
15 Portugal.  
16

17  
18 <sup>b</sup> INESC Microsistemas e Nanotecnologias and IN-Institute of Nanoscience and  
19 Nanotechnology, 1000-029 Lisbon, Portugal.  
20

21  
22 <sup>c</sup> Department of Chemical and Biological Engineering, Instituto Superior Técnico, 1049-001  
23 Lisbon, Portugal.  
24

25  
26  
27 **Corresponding Author:** Guilherme N. M. Ferreira  
28

29 **Corresponding Author's address:** IBB-Institute for Biotechnology and Bioengineering,  
30 Centre for Molecular and Structural Biomedicine (CBME), University of Algarve, Campus de  
31 Gambelas, 8000-139 Faro, Portugal.  
32

33 Phone: +351 289800054; Fax: +351 289818419.  
34  
35  
36  
37  
38  
39  
40  
41  
42  
43  
44  
45  
46  
47  
48  
49  
50  
51  
52  
53  
54  
55  
56  
57  
58  
59  
60

**Abstract**

Hydrogenated amorphous silicon (a-Si:H) photosensor was explored for the quantitative detection of HIV-1 virion infectivity factor (Vif) to a detection limit in the single nanomolar. The a-Si:H photosensor was coupled with a microfluidic channel that was functionalized with a recombinant single chain variable fragment antibody. The biosensor selectively recognized HIV-1 Vif from human cell extracts.

1  
2  
3  
4  
5  
6  
7  
8  
9  
10  
11  
12  
13  
14  
15  
16  
17  
18  
19  
20  
21  
22  
23  
24  
25  
26  
27  
28  
29  
30  
31  
32  
Semiconductor technology has been used to develop integrated photosensors containing the critical components for optical detection integrated on a single chip. Such integrated chips have been shown suitable for the sensitive, rapid and real-time measurement of optical signals,<sup>1,2</sup> also leading to portability and reduced costs, which are the major factors in boosting the miniaturized biosensors uptake in the healthcare sector particularly for on-site medical diagnostics uses.<sup>3</sup> Hydrogenated amorphous silicon (a-Si:H) photosensor have been described as a portable and sensitive detection platform, offering a promising alternative to conventional optical analytical methods.<sup>4,5</sup> In particular, a-Si:H photodiodes fit perfectly for the use as integrated photosensors because of their high quantum efficiency at visible wavelengths, low dark current, suitability for low-temperature (below 250 °C) processing technology which allow the use of a wide variety of inexpensive substrates for chip manufacturing such as glass, plastic and polymers, and easy integration into chip.<sup>4,5</sup>

23  
24  
25  
26  
27  
28  
29  
30  
31  
32  
In this work, HIV-1 proteins in solution are detected by an a-Si:H photosensor, which contains an integrated a-Si:H PIN photodiode element to convert incident light into a measurable electrical current, and an optical filtering layer to discard the effect of undesired wavelengths from the excitation light. The target protein is the HIV-1 virion infectivity factor (Vif), a 23 kDa protein mainly found in the cytoplasm of HIV-1 infected cells,<sup>6</sup> which was identified as a potential target in antiviral therapy.<sup>7</sup>

33  
34  
35  
36  
37  
38  
39  
40  
41  
42  
43  
44  
45  
46  
47  
48  
49  
50  
51  
52  
53  
54  
55  
56  
57  
58  
59  
60  
As schematically represented in Fig. 1a,b,c, the chip consists of an array of twenty three 200  $\mu\text{m} \times 200 \mu\text{m}$  a-Si:H PIN photodiode sensors integrating an amorphous silicon carbon (a-SiC:H) filter.<sup>5</sup> The chip was microfabricated as described elsewhere<sup>2,5</sup> using radio frequency plasma enhanced chemical vapor deposition and reactive ion etching to pattern the device a-Si:H PIN photodiode islands. The photodiode was deposited above the bottom contact aluminum (150 nm) and is formed by 20 nm *n*-type a-Si:H, 500 nm intrinsic a-Si:H, and 20 nm *p*-type a-Si:H. An 100-nm insulating layer of silicon nitride ( $\text{SiN}_x$ ) is used as a sidewall passivation layer and allows electrical contact between the transparent 100-nm indium tin oxide (ITO) top electrode with *p*-type a-Si:H layer. Titanium tungsten (15 nm)/aluminum (150 nm) (TiW/Al) are defined as top contact lines. A 1.96  $\mu\text{m}$  thick a-SiC:H filter film with a 2.25 eV band-gap is used to block the excitation light and to transmit the fluorescent emission light to the a-Si:H. Silicon dioxide (75 nm) was used as a passivation layer to protect the chip.

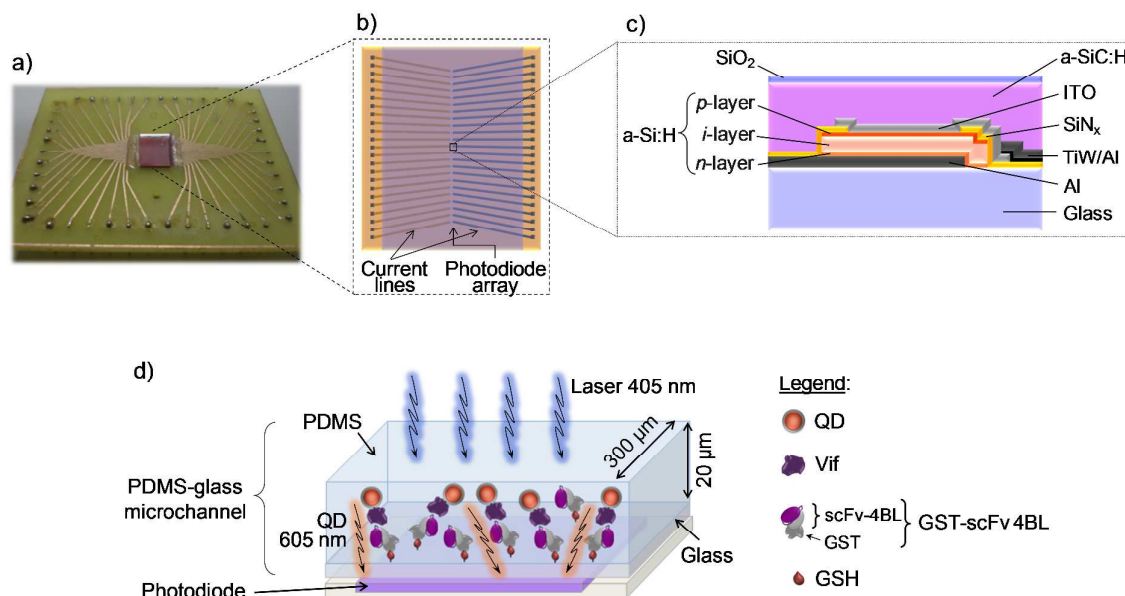


**Fig. 1** a-b) The 23-photodiode sensor chip mounted on a printed circuit board. c) Cross sectional schematic view of the a-Si:H PIN photodetector. d) Schematic of the biorecognition reactions of the probe (GST-scFv 4BL) with the target protein (Vif) labeled with quantum dots (QD) within the microchannel. a-SiC:H, amorphous silicon-carbon filter; ITO, indium tin oxide top contact, Al, aluminum bottom contact; SiN<sub>x</sub>, silicon nitride insulator film; SiO<sub>2</sub>, silicon dioxide insulator film.

The photodiodes were mounted underneath a microfluidic channel to generate the biosensor device. The microfluidic chip consists of a PDMS channel with 300  $\mu\text{m}$  in width, 20  $\mu\text{m}$  in height and 2 mm in length with one inlet and one outlet port. The channel was constructed using standard SU-8 molding and mounted on a glass slide by UV-ozone treatment sealing. The microchannel chip was functionalized with a recombinant single chain variable fragment (scFv) antibody fused to glutathione S-transferase (GST) – GST-scFv 4BL – and used to detect the target protein previously labeled with carboxyl quantum dots (QDs) 605 ITK (Invitrogen). A scheme of the use of the biosensor chip for the detection of the target proteins is shown in Fig. 1d.

The optoelectronic characteristics of the a-Si:H PIN photosensor chip<sup>8</sup> for the wavelengths of interest (405 and 605 nm) are shown in Supplementary Information. These wavelengths were chosen because they correspond respectively to the excitation and emission wavelengths of the selected QDs to fluorescently label the target HIV-1 Vif protein.

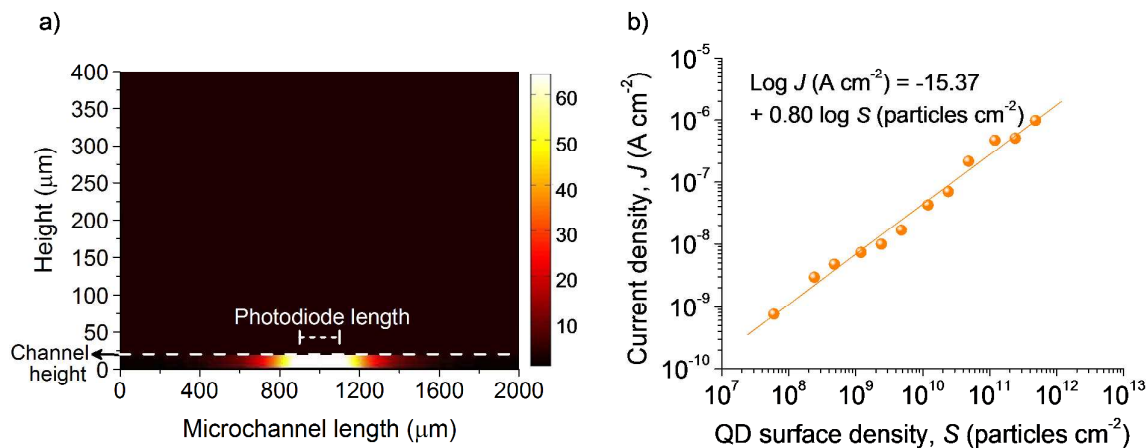


**Fig. 2** a) Scheme derived from the optical model demonstrating the zones of photons emitted by the QDs, within the microchannel, that diffuse to the detector. b) Photoresponse of the a-Si:H photosensor plotted as a function of the surface density of QDs.

As the objective of the biosensor chips is the detection of biomolecules labeled with QDs, an estimation of the amount of fluorescent light and the calibration of the photodiode response to increasing concentrations of QDs was needed. As such, the fraction of photons ( $\phi$ ) emitted by the QDs within the microfluidic channel that reaches the photodiode sensor, and thus generates a signal, was estimated from a model based on the isotropy of the emitted light.<sup>9</sup> The optical model described in Pimentel *et al.*<sup>9</sup> relates the ratio of fluorescence collected by the photodiode with the geometry of the photodiode and the relative position between the emitting species (QDs) and the photodiode. The fluorescence signal detected by a photodiode with side length  $l = 200 \mu\text{m}$ , located at a distance  $L$  from a layer of fluorescent species with a determined dimension is directly proportional to the fraction of photons reaching the device,  $\phi$ . Assuming that the photons are emitted from a distance  $L = 175 \mu\text{m}$  of the photodiode sensor, which is the average thickness of the glass used for the microfluidic chips, the fraction of photons emitted isotropically by the QDs inside the microchannel that reach the photodiode chip is  $\phi = 1.4 \times 10^{-2}$ .

In Fig. 2a is represented the scheme derived from the model that demonstrates the zones of emitted photons that reach the detector from QDs within the microchannel, as a function of the position of the photodiode (indicated as photodiode length on the scheme), and therefore contribute to the sensor signal. From all QDs within the microchannel, the main contribution to the photodiode response is given by the QDs that are over the sensor chip, as represented by the white zone in the microchannel scheme in Fig. 2a.

The photodiode signal was calibrated using solutions of 0.1 to 800 nM of QDs in Milli-Q water. The microfluidic channels were filled with the QD solutions and the sensor

1  
2  
3 photocurrent was measured after excitation with 405 nm light. The measured photocurrent  
4 was considered the fluorescence signal after removing the background signal obtained when  
5 only Milli-Q water was used. As represented in Fig. 2b, the photodiode mounted underneath  
6 the microfluidic channel chip responds linearly to the increasing concentration of QDs. The  
7 limit of detection (LOD), which establishes the lowest measured signal that can be considered  
8 significant, was set as 3-fold the standard deviation of the noise signal. For the biosensor  
9 chips herein used,  $LOD = 5.0 \times 10^7$  QDs  $cm^{-2}$  which corresponds to 80 pM was determined –  
10 the surface density of QDs was estimated by dividing the total number of QD particles in  
11 solution by the area of the microchannel top and bottom surfaces.

12  
13  
14  
15  
16  
17  
18 The functionalization of the biosensor chip, thus the immobilization of the bioreceptor  
19 molecules on the sensor surface, is a key step for the development of any biosensor.<sup>10</sup> The  
20 optimal functionalization approach must ensure high sensitivity and selectivity, which are  
21 accomplished by maximizing the density, activity and stability of the bonded bioreceptor, and  
22 by minimizing non-specific adsorption. The surface chemistry used to modify the sensor  
23 surface and the selected ligands have a critical role.<sup>10</sup> We have recently optimized a procedure  
24 to modify glass chips with silanes in which an optimal mixture of 2.5% of  
25 3-mercaptopropyltrimethoxysilane (MPTS) and a post-silanization curing process are used to  
26 maximize the surface density of chemically active thiol functions and to minimize  
27 non-specific adsorption of proteins.<sup>11</sup> After modifying the surface of the microfluidic channels  
28 with MPTS, glutathione (GSH) was covalently immobilized by incubating during 30 min a  
29 solution of GSH 33 mM in PBS pH 7.0 to generate the GSH-functionalized chips. GSH is  
30 known to enable the immobilization of biomolecules containing a GST domain via specific  
31 GST/GSH interactions.<sup>12-14</sup> On the other hand, GST is a very common domain used to label  
32 proteins by fusion techniques in molecular biology applications. We explore this GST/GSH  
33 interaction to generate a biosensor surface with highly ordered orientation of the immobilized  
34 bioreceptors. Recombinant scFv antibody – scFv 4BL – previously generated against HIV-1  
35 Vif protein<sup>15</sup> was fused to the affinity tag GST, expressed in *Escherichia coli* and purified as  
36 described in Supplementary Information. The GST-scFv 4BL fusion was further immobilized  
37 on the GSH-functionalized microchannels.

38  
39  
40  
41  
42  
43  
44  
45  
46  
47  
48  
49  
50  
51  
52  
53  
54  
55  
56  
57  
58  
59  
60  
61  
62  
63  
64  
65  
66  
67  
68  
69  
70  
71  
72  
73  
74  
75  
76  
77  
78  
79  
80  
81  
82  
83  
84  
85  
86  
87  
88  
89  
90  
91  
92  
93  
94  
95  
96  
97  
98  
99  
100  
101  
102  
103  
104  
105  
106  
107  
108  
109  
110  
111  
112  
113  
114  
115  
116  
117  
118  
119  
120  
121  
122  
123  
124  
125  
126  
127  
128  
129  
130  
131  
132  
133  
134  
135  
136  
137  
138  
139  
140  
141  
142  
143  
144  
145  
146  
147  
148  
149  
150  
151  
152  
153  
154  
155  
156  
157  
158  
159  
160  
161  
162  
163  
164  
165  
166  
167  
168  
169  
170  
171  
172  
173  
174  
175  
176  
177  
178  
179  
180  
181  
182  
183  
184  
185  
186  
187  
188  
189  
190  
191  
192  
193  
194  
195  
196  
197  
198  
199  
200  
201  
202  
203  
204  
205  
206  
207  
208  
209  
210  
211  
212  
213  
214  
215  
216  
217  
218  
219  
220  
221  
222  
223  
224  
225  
226  
227  
228  
229  
230  
231  
232  
233  
234  
235  
236  
237  
238  
239  
240  
241  
242  
243  
244  
245  
246  
247  
248  
249  
250  
251  
252  
253  
254  
255  
256  
257  
258  
259  
260  
261  
262  
263  
264  
265  
266  
267  
268  
269  
270  
271  
272  
273  
274  
275  
276  
277  
278  
279  
280  
281  
282  
283  
284  
285  
286  
287  
288  
289  
290  
291  
292  
293  
294  
295  
296  
297  
298  
299  
300  
301  
302  
303  
304  
305  
306  
307  
308  
309  
310  
311  
312  
313  
314  
315  
316  
317  
318  
319  
320  
321  
322  
323  
324  
325  
326  
327  
328  
329  
330  
331  
332  
333  
334  
335  
336  
337  
338  
339  
340  
341  
342  
343  
344  
345  
346  
347  
348  
349  
350  
351  
352  
353  
354  
355  
356  
357  
358  
359  
360  
361  
362  
363  
364  
365  
366  
367  
368  
369  
370  
371  
372  
373  
374  
375  
376  
377  
378  
379  
380  
381  
382  
383  
384  
385  
386  
387  
388  
389  
390  
391  
392  
393  
394  
395  
396  
397  
398  
399  
400  
401  
402  
403  
404  
405  
406  
407  
408  
409  
410  
411  
412  
413  
414  
415  
416  
417  
418  
419  
420  
421  
422  
423  
424  
425  
426  
427  
428  
429  
430  
431  
432  
433  
434  
435  
436  
437  
438  
439  
440  
441  
442  
443  
444  
445  
446  
447  
448  
449  
450  
451  
452  
453  
454  
455  
456  
457  
458  
459  
460  
461  
462  
463  
464  
465  
466  
467  
468  
469  
470  
471  
472  
473  
474  
475  
476  
477  
478  
479  
480  
481  
482  
483  
484  
485  
486  
487  
488  
489  
490  
491  
492  
493  
494  
495  
496  
497  
498  
499  
500  
501  
502  
503  
504  
505  
506  
507  
508  
509  
510  
511  
512  
513  
514  
515  
516  
517  
518  
519  
520  
521  
522  
523  
524  
525  
526  
527  
528  
529  
530  
531  
532  
533  
534  
535  
536  
537  
538  
539  
540  
541  
542  
543  
544  
545  
546  
547  
548  
549  
550  
551  
552  
553  
554  
555  
556  
557  
558  
559  
560  
561  
562  
563  
564  
565  
566  
567  
568  
569  
570  
571  
572  
573  
574  
575  
576  
577  
578  
579  
580  
581  
582  
583  
584  
585  
586  
587  
588  
589  
590  
591  
592  
593  
594  
595  
596  
597  
598  
599  
600  
601  
602  
603  
604  
605  
606  
607  
608  
609  
610  
611  
612  
613  
614  
615  
616  
617  
618  
619  
620  
621  
622  
623  
624  
625  
626  
627  
628  
629  
630  
631  
632  
633  
634  
635  
636  
637  
638  
639  
640  
641  
642  
643  
644  
645  
646  
647  
648  
649  
650  
651  
652  
653  
654  
655  
656  
657  
658  
659  
660  
661  
662  
663  
664  
665  
666  
667  
668  
669  
670  
671  
672  
673  
674  
675  
676  
677  
678  
679  
680  
681  
682  
683  
684  
685  
686  
687  
688  
689  
690  
691  
692  
693  
694  
695  
696  
697  
698  
699  
700  
701  
702  
703  
704  
705  
706  
707  
708  
709  
710  
711  
712  
713  
714  
715  
716  
717  
718  
719  
720  
721  
722  
723  
724  
725  
726  
727  
728  
729  
730  
731  
732  
733  
734  
735  
736  
737  
738  
739  
740  
741  
742  
743  
744  
745  
746  
747  
748  
749  
750  
751  
752  
753  
754  
755  
756  
757  
758  
759  
760  
761  
762  
763  
764  
765  
766  
767  
768  
769  
770  
771  
772  
773  
774  
775  
776  
777  
778  
779  
780  
781  
782  
783  
784  
785  
786  
787  
788  
789  
790  
791  
792  
793  
794  
795  
796  
797  
798  
799  
800  
801  
802  
803  
804  
805  
806  
807  
808  
809  
810  
811  
812  
813  
814  
815  
816  
817  
818  
819  
820  
821  
822  
823  
824  
825  
826  
827  
828  
829  
830  
831  
832  
833  
834  
835  
836  
837  
838  
839  
840  
841  
842  
843  
844  
845  
846  
847  
848  
849  
850  
851  
852  
853  
854  
855  
856  
857  
858  
859  
860  
861  
862  
863  
864  
865  
866  
867  
868  
869  
870  
871  
872  
873  
874  
875  
876  
877  
878  
879  
880  
881  
882  
883  
884  
885  
886  
887  
888  
889  
890  
891  
892  
893  
894  
895  
896  
897  
898  
899  
900  
901  
902  
903  
904  
905  
906  
907  
908  
909  
910  
911  
912  
913  
914  
915  
916  
917  
918  
919  
920  
921  
922  
923  
924  
925  
926  
927  
928  
929  
930  
931  
932  
933  
934  
935  
936  
937  
938  
939  
940  
941  
942  
943  
944  
945  
946  
947  
948  
949  
950  
951  
952  
953  
954  
955  
956  
957  
958  
959  
960  
961  
962  
963  
964  
965  
966  
967  
968  
969  
970  
971  
972  
973  
974  
975  
976  
977  
978  
979  
980  
981  
982  
983  
984  
985  
986  
987  
988  
989  
990  
991  
992  
993  
994  
995  
996  
997  
998  
999  
1000

The performance of the antibody-functionalized microchannels to recognize Vif was evaluated with the a-Si:H photosensor. Purified Vif protein<sup>16,17</sup> was labeled with QDs by conjugation using standard EDC/NHS coupling chemistry. A phosphate buffer solution of Vif-QD conjugates was flowed into the microchannel at a flow rate of 0.5  $\mu$ L  $min^{-1}$  for 15 min. A diode laser at 405 nm was used as excitation light source and the QDs fluorescence

emission at 605 nm was measured by the a-Si:H photosensor. The current density calibration of the sensor was further used to estimate the density of emitting QDs at the sensor surface. As shown in Fig. 3a, the sensor signal intensity increases as the target HIV-1 Vif protein (conjugated with the QDs) diffuses and binds to the scFv 4BL immobilized at the sensor surface, saturating after 600 s with a measured surface density of  $1.6 \times 10^{10}$  QD-Vif molecules  $\text{cm}^{-2}$ . This surface density is statistically significant different from the QD-Vif surface density obtained for the control experiment of the non-specific interaction of Vif-QD with immobilized BSA on the microchannel –  $1.1 \pm 0.2 \times 10^9$  molecules  $\text{cm}^{-2}$  (*t*-test, *P* < 0.001). The effect of the initial concentration of HIV-1 Vif-QD conjugate in the flowing solution was also investigated. A saturation curve was measured (Fig. 3b) which was fitted to a Langmuir isotherm model to obtain the equilibrium dissociation constant  $K_D = 34 \pm 8$  nM and a maximum surface density of bonded QD-Vif  $S_{max} = 1.9 \pm 0.2 \times 10^{10}$  molecules  $\text{cm}^{-2}$  ( $R^2$  of 0.97).

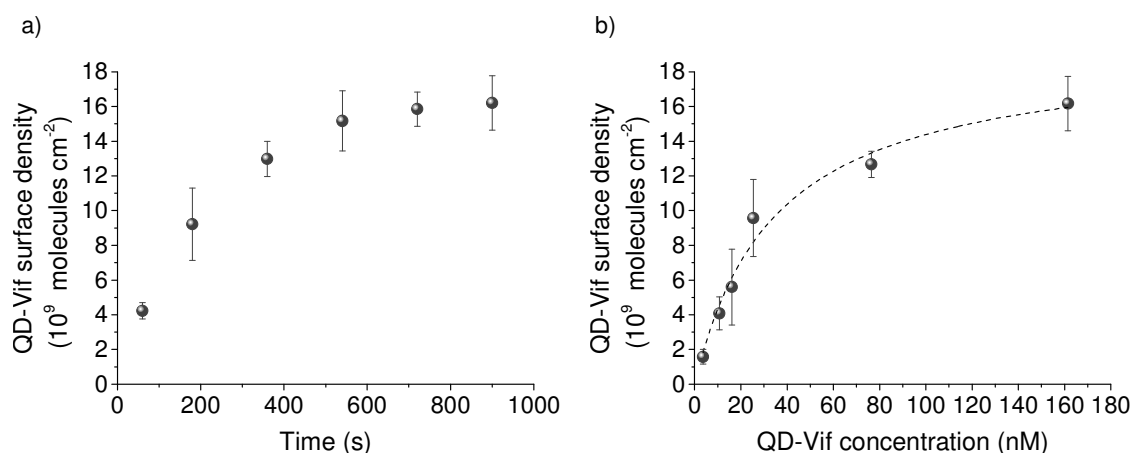


**Fig. 3** a) Surface density of captured QD-Vif by the immobilized GST-scFv 4BL as a function of flow time of QD-Vif solution. b) Surface density of captured QD-Vif by the immobilized GST-scFv 4BL as a function of the initial concentration of QD-Vif solution flowed into the channel. The dashed line is a fit to the experimental results using the Langmuir equation ( $S_{max} = 1.9 \pm 0.2 \times 10^{10}$  molecules/ $\text{cm}^2$ ,  $K_D = 3.4 \pm 0.8 \times 10^{-8}$  M,  $R^2 = 0.97$ ). The error bars are calculated from the measurements on three different samples.

The value obtained for the dissociation equilibrium constant in the nanomolar range is comparable with other affinity pairs using recombinant antibodies described in literature.<sup>18-20</sup> Moreover, when compared with previously published data obtained for the same affinity pair (scFv 4BL-Vif) on a quartz crystal microbalance immunosensor<sup>17</sup>, the  $K_D$  obtained in this work is two orders of magnitude lower, which is the result of both the higher sensitivity of the a-Si:H photosensor and of the oriented immobilization of the scFV 4BL obtained exploring the GST/GSH affinity for the immobilization, leading to higher availability of recognition



1  
2  
3 sites. The lower surface density of QD-Vif captured by the immobilized GST-scFv 4BL  
4 detected with the a-Si:H photosensor was  $1.6 \times 10^9$  molecules  $\text{cm}^{-2}$  corresponding to a  
5 QD-Vif concentration in solution of 3.6 nM, also two orders of magnitude lower than the 0.3  
6  $\mu\text{M}$  detected with the previously published QCM immunosensor.<sup>16</sup>  
7  
8

9  
10 The transport of target molecules to the surface of the activated sensor chip is a very  
11 important parameter in microfluidic chips.<sup>21,22</sup> The designed microfluidic channels must  
12 indeed ensure that enough analyte molecules are transported to the surface of the sensor  
13 where they can bind to the immobilized receptors and generate the detected signal.<sup>21,22</sup>  
14 Convection and diffusion are the two mass transport mechanisms involved in the transport of  
15 analyte molecules to the sensor surface.  
16  
17

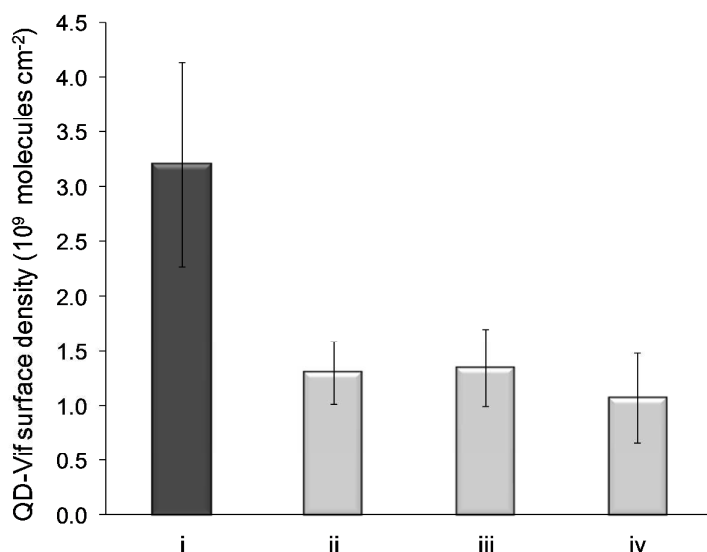
18  
19 The relative importance of mass transport by diffusion and by convection is  
20 characterized by the Péclet number,  $Pe = Q/DW$ , where  $Q$  is the flow rate,  $D$  is the diffusion  
21 coefficient of the analyte and  $W$  is the channel width. For  $Pe \ll 1$ , diffusion is faster than  
22 convection which in practical terms means that the amount of analyte reaching the sensor  
23 area, thus reacting with the immobilized biomolecules, depends on the renewal rate of the  
24 feed solution stream. On the other hand, for  $Pe \gg 1$ , convection is faster than diffusion, and  
25 analyte molecules are swept away downstream of the sensor surface before they diffuse across  
26 the channel. The diffusion coefficient for the 20-nm QD conjugate spherical particles is  
27  $2.0 \times 10^{-11} \text{ m}^2 \text{ s}^{-1}$  as estimated from the Stokes-Einstein equation. It is thus likely that the  
28 target Vif molecules labeled with the QDs will diffuse very slowly to the sensor. In fact, the  
29 Péclet number for our system at a flow rate of  $0.5 \mu\text{L min}^{-1}$  and a channel width of  $300 \mu\text{m}$ , is  
30  $Pe = 1.3 \times 10^3$ . Convective transport thus dominates over diffusive transport which means that  
31 most of the analyte molecules (bonded to the QDs) are transported away by the flow before  
32 they can diffuse to the sensor surface. Nevertheless, the few analyte molecules reaching the  
33 sensor area within the microfluidic channel will then diffuse to the sensor surface where they  
34 can react with the immobilized antibodies. In this regard, it is important to engineer the  
35 microfluidic system so that the assay is reaction limited, to guarantee that the detection is  
36 governed by the binding kinetics and that the surface concentration of analyte can be  
37 approximated to the concentration in solution. It is thus critical to compare the diffusion time  
38 versus the reaction time in order to understand if the overall binding rate is limited by the  
39 transport of analyte or by the kinetics of the binding reaction. This comparison is given by the  
40 Damköhler number,  $Da = (k_{on} S_{max} H) / D$ , where  $k_{on}$  is the association rate constant and  $H$  is the  
41 channel height.<sup>21</sup> For  $Da \gg 1$ , the system is transport limited meaning that convection and  
42 diffusion deliver analyte molecules to the sensor surface area so slowly that the binding  
43  
44  
45  
46  
47  
48  
49  
50  
51  
52  
53  
54  
55  
56  
57  
58  
59  
60

1  
2  
3 reaction can be considered instantaneous. For  $Da \ll 1$ , molecules are transported to the sensor  
4 surface faster than they can bind and the process is reaction limited. Using a dissociation rate  
5 constant ( $k_{off}$ ) previously determined using piezoelectric biosensors for the same  
6 scFv 4BL-Vif affinity pair<sup>17</sup> –  $k_{off} = 1.1 \times 10^{-3} \text{ s}^{-1}$  – the association rate constant  
7  $k_{on} = 3.2 \times 10^4 \text{ M}^{-1} \text{ s}^{-1}$  was calculated from the equilibrium constant ( $K_D = k_{off}/k_{on}$ ) obtained in  
8 this work (see above). The Damköhler number is  $Da = 9.7 \times 10^{-3}$ , which shows that this  
9 system operates in the reaction-limited regime and so the transport of analyte molecules to the  
10 sensor surface is fast enough to deliver sufficient target molecules over the surface. No  
11 analyte depletion occurs and the sensor can be used to detect and quantitatively measure the  
12 presence of HIV-1 Vif.  
13  
14  
15  
16  
17  
18  
19

20 To explore the feasibility of monitoring HIV-1 Vif using the integrated photodetector  
21 in real-life situations, we evaluated the detection of target analyte in human cell extracts. For  
22 this assay, the HIV-1 Vif produced by human embryonic kidney cell (HEK 293T) cultures  
23 was expressed as a fusion protein with the cyan fluorescent protein (CFP) to enable the  
24 monitorization of the Vif expression during cell culture by the fluorescence of the fused CFP.  
25 Not transfected cells and cells expressing only the CFP protein were used as controls.  
26 Expressed proteins were extracted from the cells after 48 h of culture and conjugated to QDs  
27 as described in Supplementary Information.  
28  
29  
30  
31  
32

33 The amount of HIV-1 Vif present in the cell extracts was  $0.15 \mu\text{M}$ , which corresponds to  
34  $9.0 \times 10^{13} \text{ molecules cm}^{-3}$ , as quantified from the CFP fluorescence measured on a Tecan  
35 Infinite M200 microplate fluorescence reader. The quantification of the total protein present  
36 in the cell extracts revealed that Vif only accounts for 0.4% of the total protein, which  
37 demonstrates the complexity of the sample. After conjugation with QDs (in which cell  
38 extracts were diluted at the concentration required for stoichiometric 1:1 Vif:QDs  
39 equivalence), the GST-scFv 4BL-functionalized microchannels were challenged with  
40 QD-labeled cell extracts. The concentration of QD-labeled cell extracts that initially flows  
41 into the microchannel, as also measured by the photosensor, was  $\sim 85 \text{ nM}$ , roughly  
42 corresponding to  $0.34 \text{ nM}$  of Vif. Microchannel chips functionalized only with GSH,  
43 therefore with no GST-scFv 4BL, were also prepared and used as control for the non-specific  
44 binding of the QD-labeled cell extracts from cells expressing Vif. As shown in Fig. 4, the  
45 detected surface density of QD-Vif from cell extracts expressing Vif was  
46  $3.2 \times 10^9 \text{ molecules cm}^{-2}$ , almost three times higher than the density obtained for the  
47 non-specific reactions with the control cell extracts –  $\sim 1.3 \times 10^9 \text{ molecules cm}^{-2}$  ( $t$ -test,  
48  $P < 0.05$ ). These results thus show the specificity of the detection and also the capability of  
49  
50  
51  
52  
53  
54  
55  
56  
57  
58  
59  
60

1  
2  
3 this microfluidic photodiode biosensor to selectively recognize HIV-1 Vif from complex  
4 cellular mixtures.  
5  
6  
7



8  
9  
10  
11  
12  
13  
14  
15  
16  
17  
18  
19  
20  
21  
22  
23  
24  
25  
26  
27  
28  
29  
30  
31  
32  
33  
34  
35  
36  
37  
38  
39  
40  
41  
42  
43  
44  
45  
46  
47  
48  
49  
50  
51  
52  
53  
54  
55  
56  
57  
58  
59  
60

**Fig. 4** Surface density of QDs obtained for the reaction of immobilized GSH/GST-scFv 4BL in the microchannel with (i) Vif-QD conjugate from cell extracts of HEK 293T expressing Vif, (ii) QDs conjugated with cell extracts obtained from cells only expressing CFP, (iii) QDs conjugated with cell extracts obtained from non-transfected cells. (iv) The non-specific reaction of immobilized GSH with Vif-QD from cell extracts expressing Vif is also shown. The error bars are calculated from the measurements on three different samples.

In summary, a microsensors, which comprises an a-Si:H PIN photodiode with an integrated a-SiC:H filter and an detachable microchannel where the biomolecules are immobilized, was used to optically detect and quantify HIV-1 Vif labeled with QDs. The influence of the initial concentration of QD-Vif in solution on the final captured analyte by the GST-scFv 4BL-functionalized surface was also investigated with the a-Si:H photosensor. The minimum surface density of QD-Vif captured by GST-scFv 4BL was  $1.6 \times 10^9$  molecules  $\text{cm}^{-2}$  which corresponds to a solution concentration in the single nanomolar range. The binding of QD-Vif with the immobilized GST-scFv 4BL followed the Langmuir model with  $K_D = 3.4 \times 10^{-8}$  M. The evaluation of detection of target analyte in complex mixtures was also performed; the methodology imposed was effective in the specific detection of HIV-1 Vif in human cell extracts. The results demonstrated the potential use of the a-Si:H photosensor as an innovative miniaturized biosensor for the diagnostics/monitoring of HIV.

## Acknowledgements

This work was supported by Fundação para a Ciência e a Tecnologia (FCT) through research project PTDC/EBB-EBI/108517, project ref. PEst-OE/EQB/LA0023/2011 and PEst-OE/CTM/LA0024/2013, and grants SFRH/BD/39278/2007, SFRH/BPD/30290/2006 and SFRH/BD/38136/2007.

## References

- 1 J. A. Chediak, Z. S. Luo, J. G. Seo, N. Cheung, L. P. Lee and T. D. Sands, *Sensor. Actuat. A-Phys.*, 2004, **111**, 1-7.
- 2 P. Novo, D. M. F. Prazeres, V. Chu and J. P. Conde, *Lab Chip*, 2011, **11**, 4063-4071.
- 3 H. Gai, Y. Li and E. S. Yeung, *Top. Curr. Chem.*, 2011, **304**, 171-201.
- 4 A. C. Pimentel, A. T. Pereira, D. M. F. Prazeres, V. Chu and J. P. Conde, *Appl. Phys. Lett.*, 2009, **94**, 164106;
- 5 A. T. Pereira, P. Novo, D. M. F. Prazeres, V. Chu and J. P. Conde, *Biomicrofluidics*, 2011, **5**, 14102.
- 6 J. Gonçalves, P. Jallepalli and D. H. Gabuzda, *J. Virol.*, 1994, **68**, 704-712.
- 7 J. L. Smith, W. Bu, R. C. Burdick and V. K. Pathak, *Trends Pharmacol. Sci.*, 2009, **30**, 638-646.
- 8 A. C. Pimentel, D. M. F. Prazeres, V. Chu and J. P. Conde, *J. Appl. Phys.*, 2009, **106**, 104904.
- 9 A. C. Pimentel, D. M. F. Prazeres, V. Chu and J. P. Conde, *J. Appl. Phys.*, 2008, **104**, 054913.
- 10 G. N. M. Ferreira, A. C. da-Silva and B. Tomé, *Trends Biotechnol.*, 2009, **27**, 689-697.
- 11 C. R. Vistas, A. C. P. Águas and G. N. M. Ferreira, *Appl. Surf. Sci.*, 2013, **286**, 314-318.
- 12 D. B. Jones, M. H. Hutchinson and A. P. Middelberg, *Proteomics*, 2004, **4**, 1007-1013.
- 13 T. H. Ha, S. O. Jung, J. M. Lee, K. Y. Lee, Y. Lee, J. S. Park and B. H. Chung, *Anal. Chem.*, 2007, **79**, 546-556.
- 14 J. S. Yuk, H-S. Kim, J-W. Jung, S-H. Jung, S-J. Lee, W. J. Kim, J-A. Han, Y-M. Kim and K-S. Ha, *Biosens. Bioelectron.*, 2005, **21**, 1521-1528.

- 1  
2  
3 15 J. Goncalves, F. Silva, A. Freitas-Vieira, M. Santa-Marta, R. Malhó, X. Yang, D.  
4 Gabuzda and C. Barbas, *J. Biol. Chem.*, 2002, **277**, 32036-32045.  
5  
6 16 G. N. M. Ferreira, J. M. Encarnação, L. Rosa, R. Rodrigues, R. Breyner, S. Barrento,  
7 L. Pedro, F. Aires da Silva and J. Gonçalves, *Biosens. Bioelectron.*, 2007, **23**, 384-392.  
8  
9 17 J. M. Encarnação, L. Rosa, R. Rodrigues, L. Pedro, F. Aires da Silva, J. Gonçalves and  
10 G. N. M. Ferreira, *J. Biotechnol.*, 2007, **132**, 142-148.  
11  
12 18 G. Zhuang, Y. Katakura, O. T., M. Kishimoto and K. Suga, *J. Biosci. Bioeng.*, 2001,  
13 **92**, 330-336.  
14  
15 19 T. Pelat, M. Hust, E. Laffly, F. Condemine, C. Bottex, D. Vidal, M. P. Lefranc, S.  
16 Dübel and P. Thullier, *Antimicrob. Agents Chemother.*, 2007, **51**, 2758-2764.  
17  
18 20 Y. Chen, K. Huang, X. Li, X. Lin, Z. Zhu and Y. Wu, *Cancer Immunol. Immunother.*,  
19 2010, **59**, 933-942.  
20  
21 21 T. Gervais and K. F. Jensen, *Chem. Eng. Sci.*, 2006, **61**, 1102-1121.  
22  
23 22 T. M. Squires, R. J. Messinger and S. R. Manalis, *Nat. Biotechnol.*, 2008, **26**, 417-426.  
24  
25  
26  
27  
28  
29  
30  
31  
32  
33  
34  
35  
36  
37  
38  
39  
40  
41  
42  
43  
44  
45  
46  
47  
48  
49  
50  
51  
52  
53  
54  
55  
56  
57  
58  
59  
60

## Table of Contents

Hydrogenated amorphous silicon (a-Si:H) photosensor is explored for the quantitative detection of HIV-1 virion infectivity factor (Vif) to a detection limit in the single nanomolar. The a-Si:H photosensor is coupled with a microfluidic channel that is functionalized with a recombinant single chain variable fragment antibody. The microfluidic biosensor selectively recognizes HIV-1 Vif from human cell extracts.

